Protein Science (1994), *3*:2089–2096. Cambridge University Press. Printed in the USA.

The role of glycine (residue 89) in the central helix of EF-hand protein troponin-C exposed following amino-terminal α-helix deletion

XIAO-LING DING, ÁRVIND BABU AKELLA, HONG SU, AND JAGDISH GULATI

The Molecular Physiology Laboratory, Division of Cardiology, Department of Medicine, Albert Einstein College of Medicine, Bronx, New York 10461

(RECEIVED May 31, 1994; ACCEPTED August 4, 1994)

Abstract

Because an N-terminal α-helical (N-helix) arm and a KGK-triplet (residues ^{88}KGK^{90}) in the central helix of troponin-C (TnC) are missing in calmodulin, several recent studies have attempted to elucidate the structure-function correlations of these units. Presently, with a family of genetically manipulated derivatives especially developed for this study and tested on permeabilized isolated single skeletal muscle fiber segments, we explored the specificities of the amino acid residues within the N-helix and the KGK-triplet in TnC. Noticeably, the amino acid compositions vary between the N-helices of the cardiac and skeletal TnC isoforms. On the other hand, the KGK-triplet is located similarly in both TnC isoforms. We previously indicated that deletion of the N-helix (mutant ΔNt) diminishes the tension obtained on activation with maximal calcium, but the contractile function is revived by the superimposed deletion of the ^{88}KGK^{90}-triplet (mutant ΔNtΔKGK; see Gulati J, Babu A, Su H, Zhang YF, 1993, *J Biol Chem 268*:11685–11690). Using this functional test, we find that replacement of Gly-89 with a Leu or an Ala could also overcome the contractile defect associated with N-helix deletion. On the other hand, replacement of the skeletal TnC N-helix with cardiac type N-helix was unable to restore contractile function. The findings indicate a destabilizing influence of Gly-89 residue in skeletal TnC and suggest that the N-terminal arm in normal TnC serves to moderate this effect. Moreover, specificity of the N-helix between cardiac and skeletal TnCs raises the possibility that resultant structural disparities are also important for the functional distinctions of the TnC isoforms.

Keywords: α-helix; calcium; calmodulin; cardiac muscle; glycine; muscle contraction; regulation; TnC structure

Troponin-C (TnC) is the Ca^{2+}-binding protein in the troponin-tropomyosin complex that switches on-off contraction. The crystal structure of the fast-twitch skeletal muscle TnC is dumbbell-shaped with 4 EF-hands (see Strynadka & James, 1989), similar to calmodulin (CaM; see Babu et al., 1988). However, whereas CaM is exceptionally multifunctional (Cohen & Klee, 1988), TnC is involved exclusively in the (skeletal and cardiac) contraction mechanism. Recent studies have probed the TnC structure in great detail to draw mechanistic insights into the Ca^{2+} switch (Grabarek et al., 1992).

Two features are self-evident. One, there is a 10–13-residue α-helix (the N-helix) at the extreme amino-terminus of TnC and this is absent in CaM. Two, the central helix is about 1 turn longer in TnC due to the extra ^{88}KGK^{90} cluster. The consequences of these have been explored by deleting either the N-helix alone (da Silva et al., 1993; Gulati et al., 1993; Smith et al., 1994) or together with the KGK-triplet (Gulati et al., 1993).

The TnC mutant with deleted N-helix has diminished contractile function because both the Ca^{2+}-activated force in the muscle fiber (Gulati et al., 1993) as well as the ATPase activity of the reconstituted acto-myosin in solution (Smith et al., 1994) are depressed. However, interestingly, the fiber contractility is restored with the double mutant deleting both the N-helix and the ^{88}KGK^{90} tripeptide (Gulati et al., 1993), indicating that the KGK-triplet also performs an important function in TnC. The present study aims to isolate the functionally critical residue(s) in this KGK-triplet.

Furthermore, the N-helix structure itself is variable between the cardiac and skeletal TnC isoforms (rabbit sTnC N-helix: TDQQAEARSY, bovine cTnC: DDIYKAAVEQ; see Gulati, 1993). Accordingly, we also aimed to investigate the functional

Reprint requests to: Jagdish Gulati, The Molecular Physiology Laboratory, Division of Cardiology, Department of Medicine, Albert Einstein College of Medicine, Bronx, New York 10461; e-mail: jgulati@aecom.yu.edu.

specificity of the N-helix in skeletal TnC by using 2 specially engineered chimeras in which the cardiac N-helix was substituted for the skeletal N-helix.

Results

To study the combined influences of the N-helix and the KGK-triplet, we developed 2 families of mutants of skeletal TnC as indicated in Figure 1. In one, the G or the K's were modified in combination with the deletion of N-helix. These genetic mutants created with PCR and cassette replacement techniques (Babu et al., 1992) are listed in Figure 1 as the *central helix replacement mutants*. In the second, the skeletal N-helix was replaced with the cardiac N-helix, and these constructs are indicated as the *cardiac N-terminal chimeras*.

Throughout this study, the recombinant skeletal TnC is called sTnC4 to distinguish it from the tissue sTnC. In mutated forms, sTnC4 is also abbreviated as S4. The functional characterizations of all mutants were made in situ in single fibers of rabbit psoas muscle. Typically, the fiber specimen was depleted of its endogenous TnC and then reconstituted with individual mutants or with wild-type sTnC4. The force development on maximal activation with pCa4 (see Materials and methods) was recorded both before TnC extraction (maximal force in this case called P_0) and following TnC reconstitution (force in this case noted as relative to P_0). The mutants were also checked for their Ca^{2+}-binding capabilities. The results on individual proteins are presented here.

The effect of N-terminal deletion mutant (ΔNt) on force regulation

In agreement with previous results (Gulati et al., 1993), the TnC-extracted fibers reconstituted with the ΔNt mutant (see Materials and methods) generate submaximal tension (45 ± 2% P_0, $n = 26$; see also Gulati et al. [1993][1]) on activation with maximal Ca^{2+} (100–300 μM free Ca^{2+}). The isolated ΔNt mutant has normal Ca^{2+}-binding capacity (3.8 ± 0.1 mol Ca^{2+}/mol ΔNt, $n = 9$; compared with 3.9 ± 0.1 mol Ca^{2+}/mol wild-type sTnC4, $n = 6$; see *precursor proteins* in Table 1).

To check whether the diminished Ca^{2+}-activated force with the ΔNt mutant might have been the consequence of incomplete loading of the protein in the TnC-extracted fiber, we returned the ΔNt-reconstituted fiber to a fresh protein-loading solution containing sTnC4 (1 mg/mL), for as long as 4 h. This resulted in no further increment in tension response (Fig. 2A), indicating that the mutant was firmly anchored in the fiber and occupied all places vacated during the extraction. Moreover, in SDS-PAGE analysis (Fig. 2B), the ΔNt-loaded fiber is estimated to have a ΔNt amount equal to the amount of endogenous tissue TnC depleted during extraction. This amount was also equal to the amount of sTnC4 in the fiber that had been extracted and straightaway loaded with wild-type sTnC4 (Table 2). Therefore, the diminished maximal tension with ΔNt occurs despite normal Ca^{2+}-binding capacity as well as normal strength of the interaction of the mutant subunit to other troponin subunits in the thin filament.

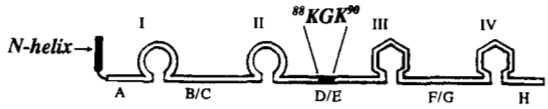

protein	N-helix residues 1-10	^{88}KGK^{90} triplet
Precursor proteins:		
tissue sTnC	^{1}TDQQAEARSY^{10}	KGK
sTnC4	A^{1}TDQQAEARSY	KGK
ΔNt	----------	KGK
ΔNtΔKGK	----------	---
Central-helix replacement mutants:		
S4•KLK	ATDQQAEARSY	KLK
ΔNt•KLK	----------	KLK
S4•KAK	ATDQQAEARSY	KAK
ΔNt•KAK	----------	KAK
S4•LGL	ATDQQAEARSY	LGL
ΔNt•LGL	----------	LGL
Cardiac N-terminal chimeras:		
cNt	ADDIYKAAVEQ	KGK
cNtΔKGK	ADDIYKAAVEQ	---

Fig. 1. Descriptions of the bacterially synthesized derivatives ΔNt and ΔNtΔKGK, as well as others generated in this study. Also depicted is a helix-loop-helix representation of the TnC molecule to highlight major features. sTnC4: wild-type sTnC. The shaded areas under the descriptions indicate the mutated regions; dashes denote when the corresponding amino acids were deleted.

The combined deletions of the N-helix from the amino-terminus and the triplet ^{88}KGK^{90} from the central helix region of the TnC molecule (double mutant ΔNtΔKGK) restored the Ca^{2+}-activated tension response in the fiber (91 ± 1% P_0; $n = 15$). The SDS-PAGE runs, similar to those in Figure 2, on fibers loaded with the double mutant indicated normal loading. To further investigate the differences between these mutants, far-UV circular dichroism measurements were made in the 200–250-nm wavelength range for sTnC4, ΔNt, and ΔNtΔKGK proteins. Additionally, at 222 nm, the temperature-dependent unfolding of these proteins were monitored. The far-UV CD spectra (between 200–250 nm) at 25 °C were found to be indistinguishable among the 3 proteins (data not shown), indicating that any structural differences between these proteins were separate from helical foldings under physiological conditions. The ellipticity estimates at 222 nm were made from the CD spectra and indicated 35–45% α-helicity in EDTA, increasing to 58% in saturating Ca^{2+} (300 μM). These findings are in agreement with the corresponding values on tissue sTnC and sTnC4 in previous

[1] The 45% tension recovery compared with 64% in Gulati et al. (1993) is partly the consequence of TnC-extraction differences: 5% P_0 presently (see Materials and methods) versus 15% P_0 in Gulati et al. (1993).

Table 1. *Tension responses with TnC mutants and ^{45}Ca-binding to purified proteins in maximal calcium solution*[a]

Proteins	Tissue TnC	sTnC4	Precursor proteins ΔNt	Precursor proteins ΔNtΔKGK	Central-helix mutants S4·KLK	Central-helix mutants ΔNt·KLK	Central-helix mutants S4-KAK	Central-helix mutants ΔNt·KAK	Central-helix mutants S4·LGL	Central-helix mutants ΔNt·LGL	N-helix chimeras cNt	N-helix chimeras cNtΔKGK
Tension recovery (%P_0)	92 ± 1 (4)	94 ± 3 (7)	45 ± 2 (26)	91 ± 1 (15)	97 ± 2 (4)	90 ± 2 (5)	96 ± 2 (3)	88 ± 1 (4)	94 ± 1 (4)	49 ± 3 (8)	45 ± 3 (6)	95 ± 4 (4)
Ca^{2+} bound (mol/mol)	3.8 ± 0.1 (7)	3.9 ± 0.1 (6)	3.8 ± 0.1 (9)	3.9 ± 0.1 (6)	n.d.	3.8 ± 0.1 (6)	n.d.	3.9 ± 0.1 (6)	4.2 ± 0.1 (6)	4.3 ± 0.1 (6)	4.1 ± 0.1 (6)	4.1 ± 0.1 (6)

[a] Tension responses of the extracted fibers (prior to reconstitution with the mutants) ranged from 0 to 12% P_0; n.d., not determined.

studies (Kawasaki & van Eerd, 1972; Murray & Kay, 1972; Johnson & Potter, 1978; Dobrowolski et al., 1991; Babu et al., 1993; Smith et al., 1994).

The thermal stabilities monitored by far-UV CD also at 222 nm are shown in Figure 3. In EDTA, the melting temperature T_m for sTnC4 is found to be 55 °C. The ΔNt mutant of the rabbit sTnC indicated a corresponding T_m value in EDTA at 45 °C, but in this case there was also a secondary unfolding at 20 °C (Fig. 3). Similar unfolding is also discernible for the ΔNt mutant of avian sTnC in the records of Smith et al. (1994; their Fig. 3). In ΔNtΔKGK, the major transition is held at 45 °C, similar to ΔNt; however, the secondary transition evident in ΔNt is suppressed in ΔNtΔKGK. With Ca^{2+}, the stabilities of all 3 proteins are augmented (Fig. 3), as also expected from the previous findings on sTnC (Privalov, 1979; Brezska et al., 1983; Tsalkova & Privalov, 1985). However, differences similar to those in EDTA between the unitary and binary mutants remain evident in the presence of Ca^{2+} (Fig. 3).

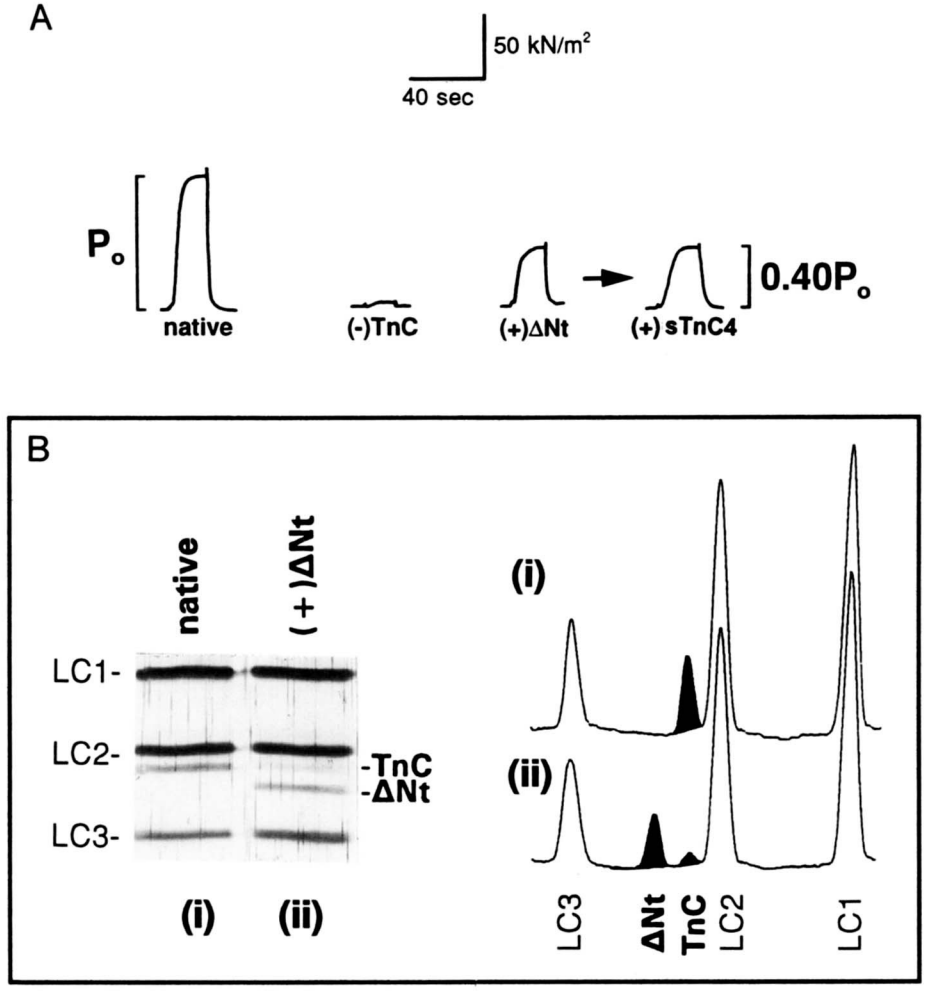

Fig. 2. A: Typical tension responses of a permeabilized muscle fiber segment with ΔNt mutant. All activations were made with 100 μM Ca^{2+} in a solution of 180 mM total ionic strength. (native: normal unextracted fiber; −TnC: the fiber following TnC extraction; ΔNt: tension response following loading the extracted fiber with the mutant). (+)sTnC4 indicates the force response following double loading the extracted fiber with ΔNt mutant and then with sTnC4. **B:** Typical gel lanes (15% polyacrylamide) and the corresponding densitometric tracings. (i) native fiber; (ii) the ΔNt reconstituted fiber. LC1–3 identify the myosin light-chain subunits. In the densitometric traces, the peaks corresponding to TnC or its variant are filled.

Table 2. *Relative intensities of TnC and mutant bands in fiber gels*

Fiber treatment	TnC/LC1	ΔNt/LC1
Native ($n = 3$)	0.21 ± 0.02	–
(+)ΔNt ($n = 3$)	0.05 ± 0.02	0.18 ± 0.01
(+)sTnC4 ($n = 5$)	0.23 ± 0.02	–

We next investigated whether the contractile functional recovery in the ΔNtΔKGK mutant was specific to the entire KGK-triplet or whether a particular residue therein was dominant in this effect.

Replacement mutants for the ^{88}KGK^{90}-triplet: The functional definition of Gly-89

A series of mutants were generated with the K and G residues of the ^{88}KGK^{90}-triplet alternately replaced by leucine (with helix-propensity) or alanine (helix-neutral), as depicted in Figure 1. The precursors for the new mutants were ΔNt and ΔNtΔKGK derivatives from the earlier study (Gulati et al., 1993). The functional properties of all mutants are shown in the composite Figure 4 and Table 1.

In the ΔNt·KLK construct, the Gly-89 residue was replaced with a leucine. For tension regulation this construct mimicked ΔNtΔKGK in the fiber, indicating that a single residue mutation within the ^{88}KGK^{90}-triplet is adequate to explain the functional recovery. The S4·KLK variant, which is the control for this, was functionally normal (force response with S4·KLK: 97 ± 2% P_0, $n = 4$, compared with 94 ± 3% P_0, $n = 7$, with sTnC4; see Table 1).

To examine whether the G → L replacement was a specific requirement for the functional recovery or whether the modification in G might be nonspecific, we designed a mutant (ΔNt·KAK) with G → A replacement. The results are shown in the bar diagram (Fig. 4) for ΔNt·KAK. The force response with maximal Ca^{2+} activation was 88 ± 1% P_0 ($n = 4$). Using the complementary control mutant S4·KAK, the tension response was 96 ± 2% P_0 ($n = 3$). Evidently, the ΔNt·KAK mimicked the double mutant ΔNtΔKGK. We conclude that the G → A replacement in the KGK tripeptide is nearly as effective as the G → L replacement. These findings suggest that the presence of Gly-89 residue is dominantly disruptive following the deletion of N-helix in the ΔNt derivative.

This attribute of the Gly-89 residue was further investigated with a new variant, ΔNt·LGL, wherein the G residue was retained but both K residues (^{88}K and ^{90}K) were changed concomitantly to L. The mutant (ΔNt·LGL) behaves similarly to the ΔNt mutant and not to ΔNtΔKGK (Fig. 4). This is the expected result if the presence of the G residue within the ^{88}KGK^{90} cluster had been primarily instrumental in producing the structural modifications that were balanced by the N-helix in the wild-type sTnC4. The control for this study was an S4·LGL construct, which with maximal Ca^{2+} maintained the permeabilized fiber functionality similar to the wild type (94 ± 1% P_0, $n = 4$).

The Ca^{2+}-binding capacities of the KGK-replacement mutants measured routinely in saturating Ca^{2+} solutions (free Ca^{2+} 300 μM) are indicated in Table 1. In every instance noted the maximum Ca^{2+} binding was preserved close to 4 mol/mol protein corresponding to the wild type.

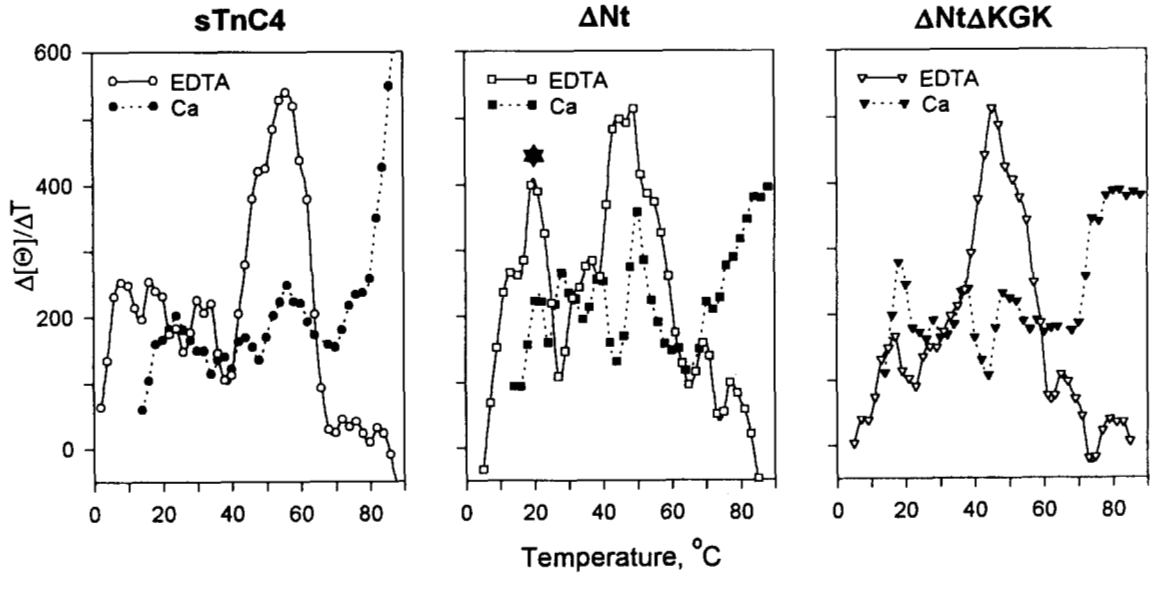

Fig. 3. Thermal unfolding of wild-type, ΔNt, and ΔNtΔKGK TnC. The ellipticity was measured as a function of temperature between 2 and 85 °C at 222 nm. The first derivative of the unfolding curves are shown. θ is in units of deg·cm^2/dmol. Open symbols, with EDTA; filled symbols, with Ca^{2+}. In EDTA, the melting temperature T_m for sTnC4 was 55 °C, and the corresponding values for the mutants were 45 °C (ΔNt) and 44 °C (ΔNtΔKGK). Note also a prominent secondary unfolding of ΔNt at the T_m of 19 °C (marked with *). This secondary unfolding is noticeably suppressed in Ca^{2+}.

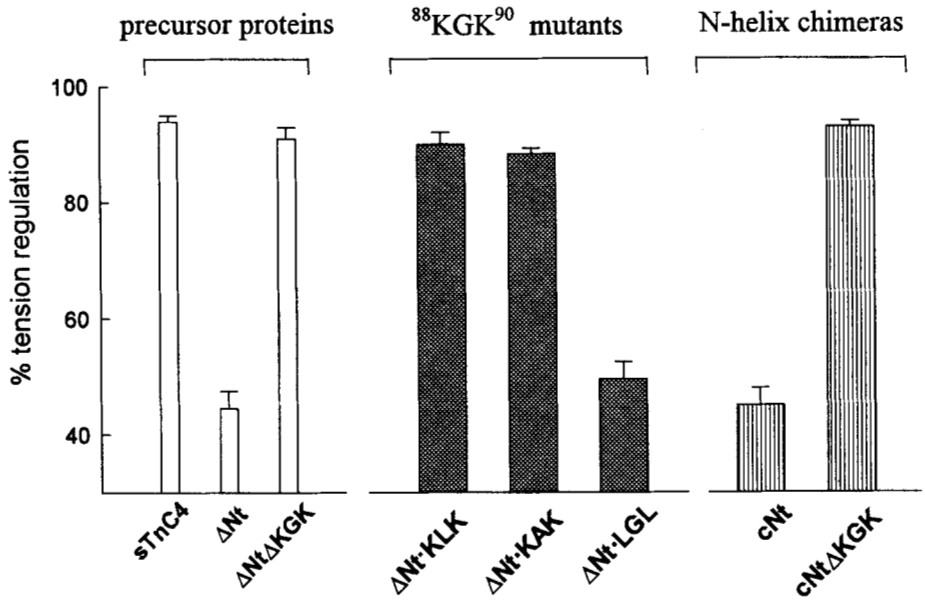

Fig. 4. The tension response of the $^{88}KGK^{90}$ replacement mutants and cardiac N-helix mutants. All data were normalized to the force (P_0) of the unextracted native fiber in 100 μM free Ca^{2+}. Each bar represents the mean and SEM of at least 4 measurements. Total of 68 fibers were used in these studies. The proteins used for the open bars are similar to before (Gulati et al., 1993).

Sequence specificity of the N-terminal arm: Cardiac N-helix chimera

To study the specificity of the N-terminal arm we engineered a mutant of sTnC in which the entire skeletal type N-helix was replaced with the N-helix of (bovine) cardiac TnC (putative cNt; see Fig. 1). We wanted to see whether this chimeric construct would perform similarly to the ΔNt derivative or alternatively whether the cardiac N-helix would adequately substitute for the skeletal N-helix. A counterpart to the double mutant ΔNtΔKGK was also made with cardiac N-helix (cNtΔKGK).

These cNt derivatives (cNt and cNtΔKGK) were checked for their Ca^{2+}-binding capacities. The results included in Table 1 (N-helix chimeras) indicate close to the expected 4 mol Ca^{2+}/mol protein. The contractile responses of the permeabilized muscle fibers with these constructs are also depicted in Figure 4. The force response in the fiber to Ca^{2+} activation of the cNt mutant is seen to be similar to the force response with ΔNt mutant, and that of the cNtΔKGK is close to the response with wild type. Thus, in both variants the presence of cNt mimics the functional characteristics associated with N-helix deletion.

Discussion

The present study explores the structure–function correlates of the N-helix together with the possible role of a $^{88}KGK^{90}$-triplet in the central helix of TnC. The findings have for the first time yielded direct insights into the mechanism of Gly-89 in the Ca^{2+} switch for contractility in rabbit fast-twitch skeletal muscle. Because typically the Gly residue in proteins serves as a strategic helix breaker (Richardson & Richardson, 1989), our findings suggest that the N-terminal arm in wild-type TnC may have evolved in part to counterbalance the destabilizing influence of Gly-89 in the central helix to shape an optimal conformation for the TnC–TnI complex for the contractile switch.

In our binary mutants, the functional recovery with selectively targeted replacements of the Gly-89 residue (G → L in ΔNtΔKLK as well as in G → A in ΔNtΔKAK), similar to that obtained with deletion of the entire $^{88}KGK^{90}$ cluster (ΔNtΔKGK), suggested that a direct interaction was possible between the N-terminal arm and the $^{88}KGK^{90}$ region. The paradoxical finding that maximal tension response was normal with a unitary ΔKGK derivative (Sheng et al., 1991; Gulati et al., 1993) might be explained if the N-terminal arm redirected its interaction to another region of the central helix. An alternative explanation of the present findings is that the N-helix deletion caused an allosteric perturbation in the protein structure and that this was also necessary to expose the observed influence of Gly-89 in the central helix. Evidently, the N-helix acts synergistically with Gly-89 to generate an optimal target-ready conformation. Moreover, our finding that the N-helix deletion was helpful in delineating the effect of Gly-89 should explain why this effect remained unexposed in previous studies (Reinach & Karlsson, 1988; Xu & Hitchcock-DeGregori, 1988).

The role of Gly-89 in TnC function

Glycines play a special role in many protein structures including α-helices because of their ability to assume multiple dihedral angles ϕ and ψ (Brant et al., 1967; Ramachandran & Sasisekharan, 1968; Hecht et al., 1986). But in α-helices, generally glycines predominate in the C-cap position and its occurrence in the center as in the TnC central helix is quite unusual (Levin & Garnier, 1988; Richardson & Richardson, 1988; Preissner & Bork, 1991). Glycines of this type should limit protein stability by increasing the number of conformations that are accessible to the unfolded form of the protein. Nevertheless, the KGK tripeptide is highly conserved in TnCs, and the Gly-89 (in rabbit TnC; Gly-92 in chicken TnC) is a possible point of conformational flexibility (Herzberg et al., 1986).

It is interesting that the KGK-triplet is not found in CaM, yet the CaM central helix is highly flexible, presumably to accommodate its interactions with multiple target proteins (Ikura et al., 1992; Meador et al., 1992). In comparison, the TnC central helix may be quite inflexible despite the insertion of the KGK tri-

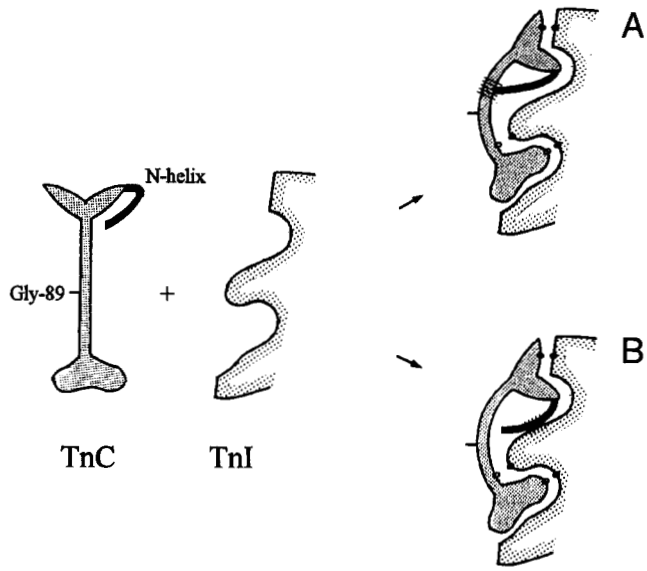

Fig. 5. The possible mechanisms of the N-helix in skeletal TnC. **A:** A direct interaction of the N-helix with the central region conduces the target ready conformation. **B:** The N-helix provides further interactions with TnI. The known interaction spots between the mainframe TnC and TnI are also noted with black circles.

peptide (Babu et al., 1993; Gulati et al., 1993). A striking explanation is that the N-helix (present in TnC and not in CaM) confers extra stability such that the resultant conformation is optimal for the contraction switch. Two relatively simple possibilities are depicted in Figure 5. In one (Fig. 5A), the N-helix is guided by Gly-89 to achieve a stable conformation in the presence of calcium. In another (Fig. 5B), in activated TnC the N-helix also interacts with TnI for the requisite conformation for contraction. In this regard it is interesting that N-helix–TnI interactions were also postulated in a recent paper by Kobayashi et al. (1994). Future studies will undoubtedly be worthwhile for exploring these possibilities in more detail. The thermal unfolding assessed by measurements of ellipticities has indicated that the ΔNt mutant may be less stable than ΔNtΔKGK and sTnC4. This would support the idea that the N-helix and Gly-89 together confer stability to the TnC structure. Similar ellipticity determinations on additional KGK-replacement mutants should be helpful in further correlating the unfolding at the melting temperatures with altered functional capabilities and for gaining insights into the specific mechanisms of these domains in the contractile switch operation.

There is also a recent report by Roquet et al. (1992) that shark α-parvalbumin contains an unusual Gly-65 at the center of the D-helix. This locus is occupied by Leu in other β-parvalbumins (see Declercq et al., 1991). The α-parvalbumin with Gly-65 corresponds to a kinked conformation of the D-helix. Because of its kinked conformation, the D-helix interacts with another part of the EF-hand protein. It is possible that this comparison with parvalbumins is relevant to the present findings on TnC.

Comparisons between the cardiac and skeletal N-helices

Finally, the inability of cardiac N-helix to substitute for skeletal N-helix is consistent with the earlier finding in which skeletal N-helix also failed to revive the cardiac Ca^{2+}-deficient EF-hand (Gulati et al., 1992). The sequences of the cardiac and skeletal N-helices vary significantly. In the X-ray structure of chicken skeletal TnC (Herzberg & James, 1988), the N-helix is stabilized by hydrophobic interactions with specific regions of Ca^{2+}-binding sites 1 and 2 in the N-terminal lobe and also by a salt bridge between Arg-11 (Arg-8 in rabbit sTnC) and Glu-76 (Glu-73 in rabbit TnC) on the D-helix of site 2. Although the cardiac N-helix exhibits a higher hydropathic index, it lacks the skeletal Arg. Also, in the remaining structure, the Glu-73 of skeletal TnC is replaced by Asp-74 in cardiac TnC. The specific requirement for the skeletal N-helix in sTnC (and conversely for the cardiac N-helix for the cardiac EF-hand; see Gulati et al., 1992) further supports the idea that Gly-89 and the N-helix function synergistically to fashion a TnC conformation that is conducive for its optimal interactions with the target protein in the Ca^{2+} switch.

In conclusion, with studies of the maximal force development both the N-helix and a middle region of the central helix in TnC are shown to play important functions in the operation of the contractile Ca^{2+} switch in muscle. This should be helpful in advancing the molecular basis of the contraction mechanism. Moreover, because cardiac TnC is identified as having a distinct length-sensing role in the heart (see Gulati, 1993), it should also be worthwhile to investigate whether the N-helix conformation influences this mechanism of the cardiac switch.

Materials and methods

Genetic manipulation of TnC: Cassette and PCR-mediated mutagenesis

The rabbit fast-twitch skeletal muscle TnC-encoding cDNA as described previously (Babu et al., 1992, 1993) was used for mutagenesis. The gene, cloned in the pT7 plasmid, included 22 unique restriction sequences to facilitate the mutagenesis. The various derivatives utilized in the present study are listed in Figure 1. The N-terminal-deleted (ΔNt and ΔNtΔKGK) mutants were the same as before (Gulati et al., 1993).

For the cNt mutant, replacing the first 12 residues, PCRs with the wild-type TnC cDNA as template was employed. The 5′ primer in this case was an 81-base oligomer with the sequence: TAAGAAGGAGATATACATATGGCTGATGATATTTATAA AGCTGCTGTTGAACAACTGACTGAAGAAATGATCGCT GAATTC. In contrast, the 5′ primer for the deletion ΔNt mutant was: AAGAAGGAGATATACATATGGCTCTGTCTGA AGAAATGA. The 3′ primer in both instances was a 42-base oligonucleotide matching the cDNA sequence for residues 62–76 of the TnC. The 228-bp PCR products were separated on a 1.5% agarose gel. The expected band was excised and the desired PCR product was released from agarose by filtering through glass wool with centrifugation (13,000 × *g* × 10 min). This was carried out in a laboratory apparatus consisting of a 2-Eppendorf tube cascade. The upper unit (0.5-mL tube) had a hole drilled at the bottom and plugged with glass wool. The excised PCR band from the agarose gel was placed on top of the glass wool plug and the filtrate was collected in the lower Eppendorf tube (2-mL tube). The final purification step involved standard ethanol precipitation of the filtrate, and the PCR product was finally inserted into the TnC plasmid between

the *Nde* I/*Sal* I sites by standard ligation procedures (Sambrook et al., 1989). The N-terminal amino acid residues of the 2 key recombinant proteins (wild type and ΔNt) for this study were also sequenced (see below).

The deletion/replacement mutations of the central helix linker were developed with appropriate oligonucleotide cassettes inserted between the *Eco* RI–*Nhe* I or *Nhe* I–*Sty* I pairs (see Babu et al., 1992). All mutant cDNAs, prior to protein expression step, were sequenced by the dideoxy sequencing procedure using a commercial kit (USB Sequenase 2.0 kit).

The bacterial expression and column purification of the recombinant proteins were as in Babu et al. (1992) (see also Gulati et al., 1993). The proteins were stored at −20 °C in 10 mM Tris, 5 mM dithiothreitol (DTT), pH 7.5. The wild-type recombinant was designated sTnC4.

A batch each of sTnC4 and ΔNt was also microsequenced at the N-terminus. The first 23 residues of the former and 13 residues of the latter were found as: ATDQQAEARSYLSEEMI AEFKAA (sTnC4) and ALSEEMIAEFKAA (ΔNt). The microsequencing was performed with an Applied Biosystems 477A protein sequencer. The determined amino acid sequences confirm the corresponding cDNA sequences except for the beginning methionine, which was evidently cleaved off in the bacterium. However, the next alanine included in the cDNA construct to help engage the bacterial translational machinery was found to be retained. This Ala ordinarily is novel for vertebrate sTnC; nevertheless, functionally in the fiber, the wild-type recombinant was indistinguishable from purified rabbit muscle TnC.

Permeabilized fibers: TnC extraction and reconstitution

The muscle fiber single segments (typically 50–150 μm wide and 2–4 mm long) were isolated from the rabbit psoas fast-twitch muscle and permeabilized as before (Gulati, 1976; Gulati et al., 1991). The fiber length between the attachments at the 2 ends was kept small (2–4 mm) to help maintain uniformity during activation. The sarcomere length following attachment was adjusted at 2.5 μm in the relaxing solution and monitored periodically with laser diffraction, throughout the experiment.

The effects of the TnC mutants on the fiber were assessed by first extracting the endogenous TnC and then repleting the extracted fiber with a desired mutant. As before (Babu et al., 1987; Gulati et al., 1991), the TnC extraction was in an EDTA solution (5 mM K_3EDTA, 10 mM imidazole, pH 7.2) at 28 °C. The maximally Ca^{2+}-activated tension following extraction was typically below 0.05 P_0 (P_0 = maximal tension of the same skinned fiber prior to extraction). The maximal Ca^{2+} activations of the rabbit fibers were routinely made at 5 °C.

For TnC repletion, the extracted fiber was incubated for 30 min in the *relaxing* solution (20 mM imidazole, 6.5 mM ATP, 5 mM EGTA, 15 mM phosphocreatine, 6 mM $MgCl_2$, 90 mM K-propionate, pH 7.0, 5 °C; 180 mM, ionic strength; modified from Gulati & Podolsky, 1978) containing approximately 1 mg/mL of the mutant TnC or the wild-type TnC (sTnC4). The fiber was next returned to the relaxing solution without the protein, to wash out any free protein. It was then activated with 100 μM Ca^{2+}. If the maximal tension following the protein treatment was significantly below P_0, the treatment with the mutant was continued for an additional 20 min. The ultimate incubation in each case was made in sTnC4 (1 mg/mL; 3–5-min exposure) to gain the assurance that the loading had been complete, otherwise the experiment was disregarded. Additional assurance whether the loading of the particular protein was complete was derived from quantitative analyses of SDS-PAGE developed from selected experimental fiber segments (see below).

SDS-PAGE analysis of the experimental fiber segments

All experimental fiber segments were stored at −20 °C for subsequent SDS-PAGE analysis. The 12% or 15% polyacrylamide minigels were used throughout. The fiber was dissolved by microtip ultrasonication in 20 μL of SDS sample buffer (62.5 mM Tris-HCl, pH 6.8, 10% [v/v] glycerol, 20% [w/v] SDS, 70 mM β-mercaptoethanol, 0.001% [w/v] bromophenol blue); 10 μL was loaded per lane and duplicate lanes were used: in one, the sample buffer contained 5 mM EGTA; in the second, 5 mM $CaCl_2$ was added. With EGTA, the fiber TnC band often comigrated with LC2 (myosin light chain 2), but the TnC and LC2 bands could be well separated by the addition of 5 mM $CaCl_2$ in the sample buffer. The silver-staining steps were essentially the same as before (Babu et al., 1987). The bands were quantitatively analyzed by laser densitometry (Ultroscan XL, equipped with a 100-μm beam; Pharmacia). The TnC and mutant amounts in each lane were normalized to LC1-intensity scanned in the same lane. LC1 was useful as the internal control because it was found to be impervious to the TnC-extraction treatments in this study. Accordingly, the results are presented as fractions of LC1 (see Babu et al., 1987).

$^{45}Ca^{2+}$-binding measurements on isolated bacterially synthesized proteins

These measurements were made on purified proteins by microdialysis in an 8-well (BRL) unit, as before (Gulati et al., 1992). The reservoir buffer (400 mL) contained 100 mM KCl, 10 mM 3-(*N*-morpholino)propanesulfonic acid, pH 7.5, with 0.3 mM $CaCl_2$ (*p*Ca 3.52) including 100 μCi of $^{45}Ca^{2+}$. The solution was run through a Chelex column prior to the addition of $CaCl_2$ and radiolabeled $^{45}Ca^{2+}$. Following 48 h of dialysis at 4 °C, the unit was maintained at room temperature for 30 min with continuing circulation (20 mL/h). Aliquots were removed for radioactivity counts to estimate Ca^{2+} binding in triplicate. The protein quantitation on each well was done in duplicate on separate aliquots using the BioRad protein assay, as described before (Babu et al., 1992).

Circular dichroism spectroscopy

CD measurements were performed on a Jasco J720 spectropolarimeter fitted with a thermal regulated cell holder in a 1-mm circular quartz cuvette. The temperature could be varied between 2 and 85 °C. The far-UV CD spectra were measured between 200 and 250 nm, every 0.5 nm, with 2-s collection times. The protein concentration was 0.2 mg/mL in 50 mM KCl, 2 mM HEPES, pH 7, 0.5 mM DTT, and either 2 mM EDTA or 3 mM $CaCl_2$. The mean residue ellipticity (θ) was determined and the α-helicity content was estimated as before according to Greenfield and Fasman (1969) (see Babu et al., 1993).

Thermal denaturation

The temperature-dependent unfolding was monitored at 222 nm. The temperature was varied between 2 and 85 °C in 2° intervals with 1-min equilibration and 2-s collection times.

Acknowledgments

We are grateful to Venu G. Rao for assistance with some of the experiments. Grants were from NIH (AR 33736) and the New York Heart Association. Part of the equipment was purchased with help from the Blumkin Fund. The Laboratory of Macromolecular Analysis assisted with microsequencing the N-terminal regions of the recombinants and also with the measurements of CD.

References

Babu YS, Bugg CE, Cook J. 1988. Structure of calmodulin refined at 2.2 Å resolution. *J Mol Biol 204*:191–204.

Babu A, Rao VG, Su H, Gulati J. 1993. Critical minimum length of the central helix in troponin C for the Ca^{2+} switch in muscular contraction. *J Biol Chem 268*:19232–19238.

Babu A, Scordilis S, Sonnenblick E, Gulati J. 1987. The control of myocardial contraction with skeletal fast muscle troponin C. *J Biol Chem 262*:5815–5822.

Babu A, Su H, Ryu Y, Gulati J. 1992. Determination of residue specificity in the EF-hand of troponin C for Ca^{2+} coordination, by genetic engineering. *J Biol Chem 267*:15469–15474.

Brant DA, Miller WG, Flory PJ. 1967. Conformational energy estimates for statistically coiling polypeptide chains. *J Mol Biol 23*:47–65.

Brezska H, Venyaminov SV, Grabarek Z, Drabikowski W. 1983. Comparative studies on thermostability of calmodulin, skeletal muscle troponin C and their tryptic fragments. *FEBS Lett 153*:169–173.

Cohen P, Klee CB. 1988. *Calmodulin, molecular aspects of cellular regulation*. New York: Elsevier.

da Silva EF, Sorenson MM, Smillie LB, Barrabin H, Scofano HM. 1993. Comparison of calmodulin and troponin C with and without its amino-terminal helix (residues 1–11) in the activation of erythrocyte Ca^{2+}-ATPase. *J Biol Chem 268*:26220–26225.

Declercq JP, Tinant B, Parello J, Rambaud J. 1991. Ionic interactions with parvalbumin: Crystal structure determination of pike 4.10 parvalbumin in four different ionic environments. *J Mol Biol 220*:1017–1039.

Dobrowolski Z, Xu GQ, Hitchcock-Degregori SE. 1991. Modified calcium dependent regulatory function of troponin C central helix mutants. *J Biol Chem 266*:5703–5710.

Grabarek Z, Tao T, Gergely J. 1992. Molecular mechanism of troponin C function. *J Muscle Res Cell Motil 13*:383–393.

Greenfield N, Fasman GD. 1969. Computed circular dichroism spectra for the evaluation of protein conformation. *Biochemistry 8*:4108–4116.

Gulati J. 1976. Force-velocity characteristics of calcium activated slow and fast twitch mammalian fibers from the guinea pig. *Proc Natl Acad Sci USA 73*:4693–4697.

Gulati J. 1993. Molecular biology of the length-tension relation in cardiac muscle. In: Sugi H, Pollack GH, eds. *Mechanism of myofilament sliding in muscle contraction*. New York: Plenum. pp 593–602.

Gulati J, Babu A, Su H. 1992. Functional delineation of the Ca^{2+} deficient EF-hand in cardiac muscle, with genetically engineered cardiac-skeletal chimeric troponin C. *J Biol Chem 267*:25073–25077.

Gulati J, Babu A, Su H, Zhang YF. 1993. Identification of the regions conferring calmodulin-like properties to troponin C. *J Biol Chem 268*: 11685–11690.

Gulati J, Podolsky RJ. 1978. Contraction transients of skinned fibers. Effects of calcium and ionic strength. *J Gen Physiol 72*:701–716.

Gulati J, Sonnenblick E, Babu A. 1991. The role of troponin C in the length dependence of Ca^{2+} sensitive force of mammalian skeletal and cardiac muscles. *J Physiol (Lond) 441*:305–324.

Hecht MH, Sturtevant JM, Sauer RT. 1986. Stabilization of λ repressor against thermal denaturation by site-directed Gly → Ala changes in α-helix 3. *Proteins Struct Funct Genet 1*:43–46.

Herzberg O, James MNG. 1988. Refined crystal structure of troponin C from turkey skeletal muscle at 2.0 Å resolution. *J Mol Biol 203*:761–779.

Herzberg O, Moult J, James MNG. 1986. Calcium binding to skeletal muscle troponin C and the regulation of muscle contraction. *Ciba Found Symp 122*:120–144.

Ikura M, Clore GM, Gronenborn AM, Zhu G, Klee CB, Bax A. 1992. Solution structure of a calmodulin-target peptide complex by multidimensional NMR. *Science 256*:632–638.

Johnson JD, Potter JD. 1978. Detection of two classes of Ca^{2+}-binding sites in troponin C with circular dichroism and tyrosine fluorescence. *J Biol Chem 253*:3775–3777.

Kawasaki Y, van Eerd JP. 1972. The effects of Mg^{2+} on the conformation of the Ca^{2+}-binding component of troponin. *Biochem Biophys Res Commun 47*:859–864.

Kobayashi T, Tao T, Gergely J, Collins JH. 1994. Structure of troponin complex: Implications of the photocross-linking of troponin I to troponin C thiol mutants. *J Biol Chem 269*:5725–5729.

Levin JM, Garnier J. 1988. Improvements in a secondary structure prediction method based on a search for local sequence homologies and its use as a model building tool. *Biochim Biophys Acta 955*:283–295.

Meador WE, Means AR, Quiocho FA. 1992. Target enzyme recognition by calmodulin: 2.4 Å structure of a calmodulin–peptide complex. *Science 257*:1251–1255.

Murray AC, Kay CM. 1972. Hydrodynamic and optical properties of troponin A. Demonstration of conformational changes upon binding calcium ion. *Biochemistry 11*:2622–2627.

Preissner R, Bork P. 1991. On α-helices terminated by glycine. 1. Identification of common structural features. *Biochem Biophys Res Commun 180*:660–665.

Privalov PL. 1979. Stability of proteins. Small globular proteins. *Adv Protein Chem 33*:167–241.

Ramachandran GN, Sasisekharan V. 1968. Conformation of polypeptides and proteins. *Adv Protein Chem 23*:283–437.

Reinach FC, Karlsson R. 1988. Cloning, expression, and site-directed mutagenesis of chicken skeletal muscle troponin C. *J Biol Chem 263*:2371–2376.

Richardson JS, Richardson DC. 1988. Amino acid preferences for specific locations at the ends of α-helices. *Science 240*:1648–1652.

Richardson JS, Richardson DC. 1989. Principles and patterns of protein conformation. In: Fasman GD, ed. *Predictions of protein structure and the principles of protein conformation*. New York: Plenum Press. pp 1–98.

Roquet F, Declercq JP, Tinant B, Rambaud J, Parello J. 1992. Crystal structure of the unique parvalbumin component from muscle of the leopard shark (*Triakis semifasciata*): The first X-ray study of an α-parvalbumin. *J Mol Biol 223*:705–720.

Sambrook J, Fritsch JM, Maniatis T. 1989. *Molecular cloning*. Cold Spring Harbor, New York: Cold Spring Harbor Laboratory Press.

Sheng Z, Francois JM, Hitchcock-DeGregori SE, Potter JD. 1991. Effects of mutations in the central helix of troponin C on its biological activity. *J Biol Chem 266*:5711–5715.

Smith L, Greenfield NJ, Hitchcock-DeGregori SE. 1994. The effects of deletion of the amino-terminal helix on troponin C function and stability. *J Biol Chem 269*:9857–9863.

Strynadka NCJ, James MNG. 1989. Crystal structures of the helix-loop-helix calcium-binding proteins. *Annu Rev Biochem 58*:951–998.

Tsalkova TN, Privalov PL. 1985. Thermodynamic study of domain organization in troponin C and calmodulin. *J Mol Biol 181*:533–544.

Xu GQ, Hitchcock-DeGregori SE. 1988. Synthesis of troponin C cDNA and expression of wildtype and mutant proteins in *E. coli*. *J Biol Chem 263*:13962–13969.